Applied Physics A (2024) 130:241
https://doi.org/10.1007/s00339-024-07403-z

Applied Physics A
Materials Science & Processing

Investigating spectral enhancement of monolayer MoS_2 coupled with Ag nanowires gap-mode surface plasmons

Weibin Zhang[1] · Cunwei Kong[1] · Chunming Ji[1] · Xinfeng Zhang[1,2] · Quan Wang[1,3]

Received: 2 August 2023 / Accepted: 21 February 2024

Abstract
The combination with surface plasmons (SPs) nanostructures is an effective method to improve the optical properties of two-dimensional (2D) materials such as molybdenum disulfide (MoS_2). Silver nanowire (Ag NW) is one of the most important SPs materials because of its tunable SPs resonance characteristics from visible light to near-infrared light. SPs can effectively confine the light field to the nanometer scale for propagation and localization, breaking the limit of optical diffraction, and the distribution of its electromagnetic field often depends on the dielectric environment. The existence of the gap-mode SPs makes the electromagnetic field between the Ag NWs coupled, so the double Ag NWs can produce additional electromagnetic field enhancement than the single Ag NW. Here, the gap-mode SPs of two different positional relationships of Ag NWs were studied through theoretical simulation, and the increase in the field enhancement factor was obtained as a function of gap distance. It is experimentally confirmed that the Raman and photoluminescence intensities of monolayer MoS_2 are enhanced by the coupling of gap-mode SPs, and the effects of doping and stress are excluded. The results are helpful to better understand the gain mechanism of gap-mode SPs on the optical properties of 2D materials, and provide a reference for the design of new SPs nanostructures.

Keywords Gap-mode surface plasmons · Ag nanowires · Monolayer molybdenum disulfide · Photoluminescence · Raman spectroscopy

1 Introduction

Two-dimensional (2D) molybdenum disulfide (MoS_2) has good physical properties and is one of the promising materials for the development of high-performance and low-power electronic components [1–10]. 2D MoS_2 can be used as a channel material to fabricate field effect transistors (FET) with high carrier mobility and high switching ratio ($> 10^7$) [10], which is expected to replace traditional silicon-based FETs due to the adjustable band gap in the range of 1.2–1.8 eV [3, 4]. Moreover, 2D MoS_2 has a good response to light and has application prospects in future optoelectronic devices [7–9]. However, the atomic thickness limits the optical absorption cross-section of 2D MoS_2, which is one of the key problems hindering its application in optoelectronic devices [11–13].

Surface plasmon (SP) is a coherent collective oscillation of metal conduction band electrons excited by incident light, which can form a strong local electric field enhancement under resonance excitation [14]. The SPs excited on the metal nanostructures can break through the optical diffraction limit and realize the localization of the light field on the micro-nano scale [15, 16]. At present, SPs nanostructures have been widely used to enhance the interaction between light and matter. By combining with SPs nanostructures, the photoelectric properties of 2D materials can be effectively improved [17–21].

However, in the composite system of single silver nanowire (Ag NW) and monolayer MoS_2, only the localized surface plasmons (LSPs) are produced. Unlike the propagating surface plasmons (PSPs) that can propagate along the interface between the metal and the medium,

✉ Quan Wang
wangq@ujs.edu.cn

[1] Zhenjiang Key Laboratory of Advanced Sensing Materials and Devices, School of Mechanical Engineering, Jiangsu University, Zhenjiang 212013, People's Republic of China

[2] Jiangsu Zorrun Semiconductor Co., Ltd, Nantong 226500, China

[3] State Key Laboratory of Transducer Technology, Chinese Academy of Sciences, Shanghai 200050, China

Published online: 22 March 2024

LSPs only forms a locally enhanced electromagnetic field. The LSPs are concentrated at the interface between the metal–dielectric interface, resulting in the weak localization and enhancement of the light field by Ag NW SPs. Fortunately, under appropriate excitation conditions, the SPs of the nanostructures close to each other will be coupled. This coupling leads to a greater enhancement of the electric field at the gap of the nanostructures, and the intensity is higher than that of single nanostructure [22–28]. Wu et al. [22] sandwiched a monolayer (1L) MoS_2 between Ag nanoparticles and Au substrate, which increased the photoluminescence (PL) intensity of the 1L MoS_2 by a factor of 110. Sun et al. [23] constructed a photodetector based on Ag nanocube-1L MoS_2-Ag film. The photoresponsivity of the device reached 7940 A/W, which was 38 times that of the original MoS_2 photodetector under the same parameters. Hao et al. [25] enhanced the PL intensity of 1L MoS_2 by 160 times by constructing a composite structure of metal nanostructured dimers and 1L MoS_2. Lee et al. [27] integrated 1L MoS_2 with a silver-necked nanoantenna array, and the enhanced exciton-plasmon coupling led to profound changes in the emission and excitation processes, resulting in a significant enhancement of the PL spectrum. Therefore, it is necessary to explore the coupling mechanism of this nanostructured gap-mode SPs in order to better understand the gain mechanism of gap-mode SPs on the optical properties of 2D materials.

In order to study the SPs coupling mode between Ag NWs, we will explore the coupling mechanism of Ag NW gap mode SPs through optical simulation and spectral enhancement experiment of monolayer MoS_2 by double Ag NWs. Here, the electric field distribution of double Ag NWs at different gap distances was simulated. In addition, the Raman and PL intensities of monolayer MoS_2 enhanced by double Ag NWs cross-excited SPs were experimentally studied.

2 Simulation and experimental details

2.1 FDTD calculation method

In the finite difference time domain (FDTD) simulation process, the light source selects the full-field scattered field light, and the boundary conditions in the X, Y, and Z directions are set to the perfect matching layer (PML). The grid accuracy is set to 0.1 nm, the simulation duration is set to 1000 fs, and the diameter of Ag NWs is set to 45 nm. In free space, the SPs electric field distribution of single Ag NW and double Ag NWs under different gap distances is simulated. The gap distances are set to 75 nm, 30 nm, 10 nm, 2 nm and 0.6 nm, respectively.

2.2 Experimental method

A monolayer MoS_2 sample was grown on a silicon substrate with oxide layer thickness of 300 nm by CVD method. Ag NWs with an average diameter of 20 nm were synthesized by reducing $AgNO_3$ in ethylene glycol by polyol method. The MoS_2/Ag (Ag NWs are buried under the MoS_2 film) composite structure was constructed by spin-coating Ag NW solution on a blank substrate using PMMA-assisted wet transfer technology, As shown in Fig. 1a. In order to construct Ag/MoS_2 (Ag NWs are stacked on top of the MoS_2 film) composite structure, we directly spin-coated Ag NW solution on the substrate containing 1L MoS_2 sample.

2.3 Raman and PL spectroscopy

Raman and PL spectra were measured using a laser with a wavelength of 532 nm on a multi-functional integrated test platform (Metatest, ScanPro Advance). The principle of spectral measurement is shown in Fig. 1b. The measured power of Raman and PL spectra were set to 1 mW and 0.5 mW, respectively. All measurements are taken at room temperature.

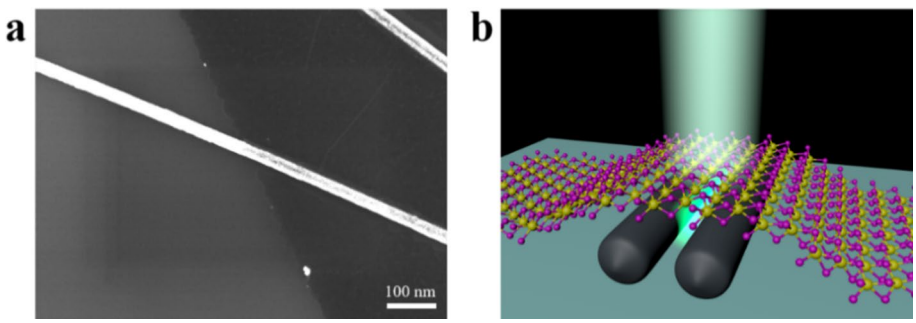

Fig. 1 **a** SEM image of MoS_2/Ag composite structure. **b** Spectrogram of spectral measurement

3 Results and discussion

The SPs distributions of double Ag NWs with different gap distances in free space are shown in Fig. 2a and b–f, respectively. The light field is effectively confined to the nanometer scale, and the SPs of single Ag NW are symmetrically distributed around it. As the gap distance (L_g) between the double Ag NWs decreases, the coupled SPs will gradually concentrate in the gap. When L_g is less than 10 nm, the electric field intensity on both sides of the double Ag NWs is significantly weaker than that in the gap region.

The field enhancement factor in this paper is defined as $|E|/|E_0|$, where $|E_0|$ is the set initial electric field intensity, and $|E|$ is the electric field intensity enhanced by the gap-mode SPs. From Fig. 2b–f, it can be seen that the electric field enhancement of double Ag NWs increases with the decrease of gap distance under the action of gap mode SPs. When gap distance is less than 10 nm, the electric field intensity on both sides of the double Ag NWs begins to be significantly weaker than that in the middle gap region. It can be seen from Fig. 2f that when gap distance is equal to 0.6 nm, the field enhancement factor in the gap region can reach more than 70, which is much higher than the maximum field enhancement factor of single Ag NW. This shows that the gap-mode SPs of double Ag NWs can not only concentrate the light in a smaller region, but also couple a strong and tunable electric field. From Fig. 2, the

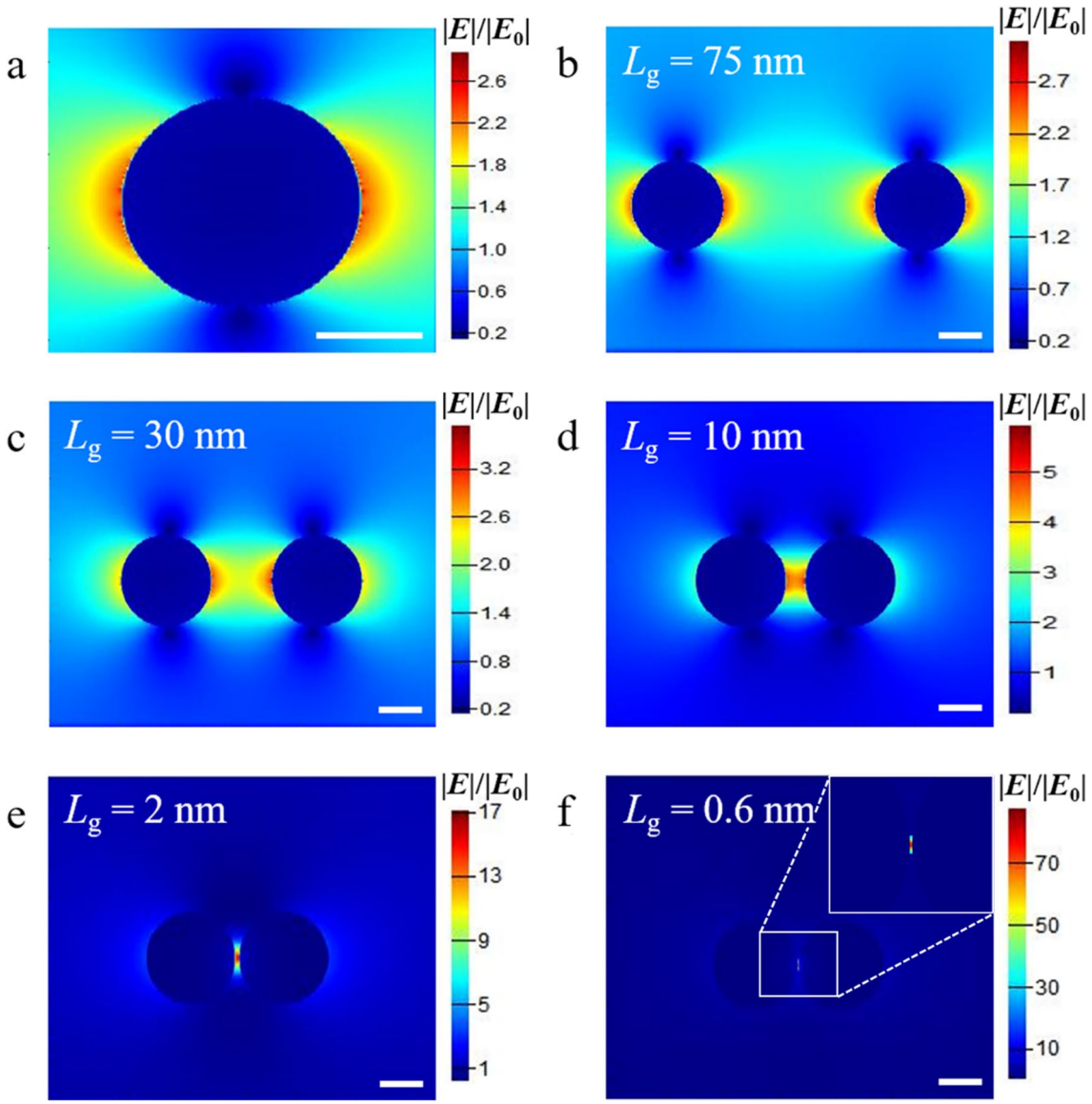

Fig. 2 FDTD simulation of the SPs electric field distribution. **a** SPs of a single Ag NW. **b–f** SPs of two nearly parallel Ag NWs with different gap distances. All scales are 20 nm

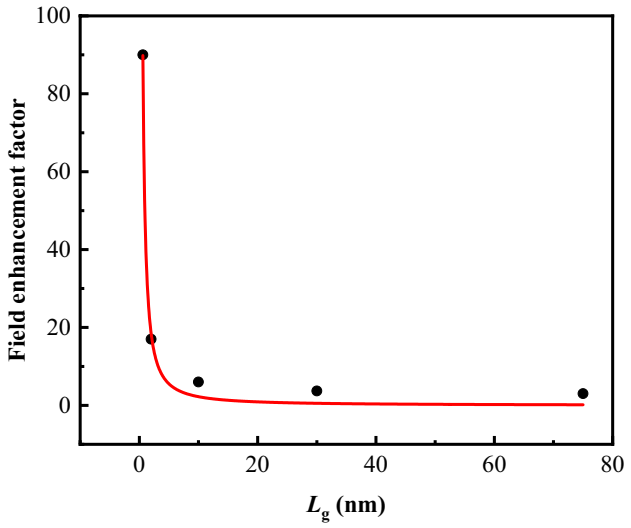

Fig. 3 The function curve of field enhancement factor increasing with the decrease of gap distance

function that the field enhancement factor increases with the decrease of the gap distance can be obtained, and the fitting curve is shown in Fig. 3.

Then, parallel and intersecting double Ag NWs and the MoS_2/Ag composite structures with monolayer MoS_2 were prepared. By comparing the Raman spectral intensities at the nanowires' gap and surrounding points, it can be inferred that the SPs light field enhancement degree of these points and whether there is a gap mode "hot spot". This is helpful to further verify the existence of the Ag NWs gap mode SPs. Figure 4a shows the positions of the three spectral collection points on the MoS_2/Ag composite structure. The angle between the two NWs is less than 3 degrees, that is, they are almost parallel. Point 1 is located in the middle of double Ag NWs, and the spectral intensity of this point can be enhanced by the gap-mode SPs. Point 2 is located on the side of the Ag NWs, and the spectral intensity of this point can only be enhanced by single Ag NW SPs. Point 3 is located far away from the parallel Ag NWs, representing the optical properties of intrinsic MoS_2. The corresponding PL and Raman spectra of the three points are shown in Fig. 4b, c, respectively. When the laser is irradiated in the gap of NW,

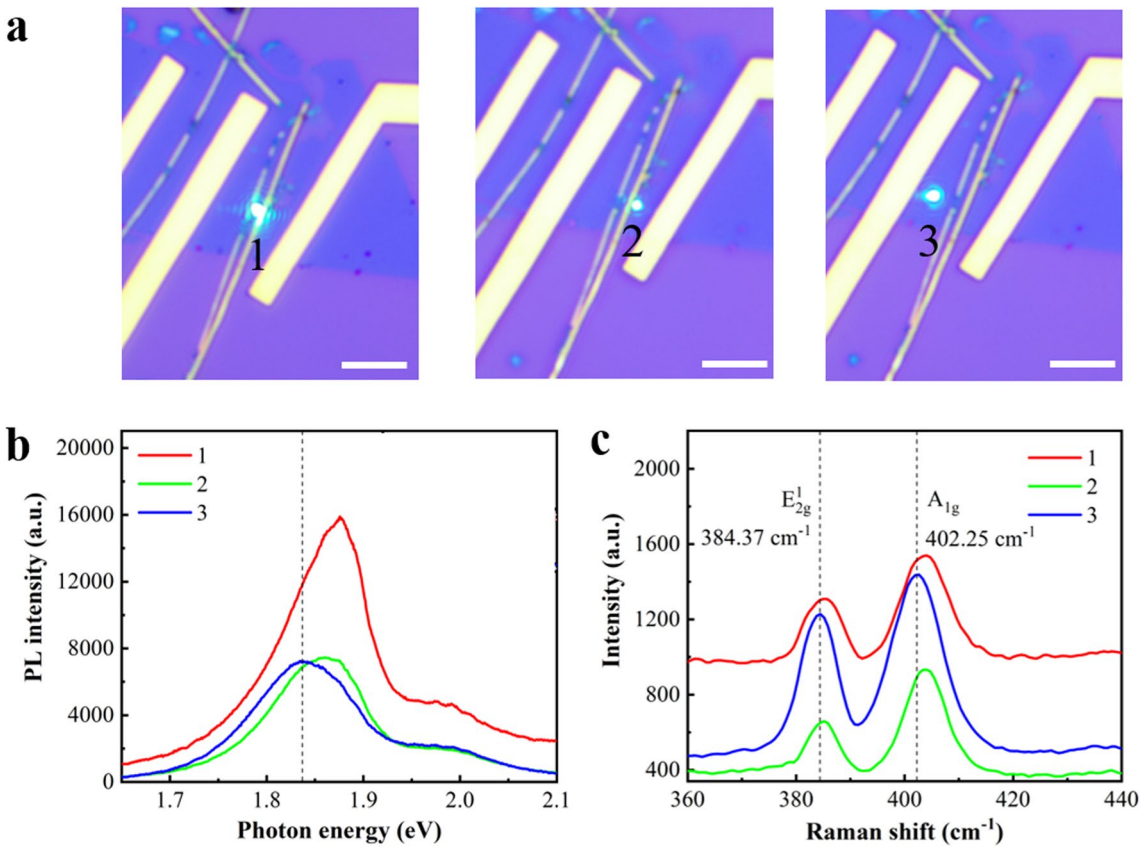

Fig. 4 Spectral enhancement of double Ag NWs in the MoS_2/Ag composite structure. **a** Locations of the spectrum collection points. All scales are 5 μm. **b** Comparison of PL spectra. Illustrations show that the PL spectra of positions 1 and 3 are fitted by Lorentz function. **c** Comparison of Raman spectra

the PL intensity of MoS_2 is enhanced by two times compared with the other two points, indicating that a stronger SP is excited. When the laser is irradiated on the side of the Ag NWs, no spectral enhancement is observed, indicating that the light field after SPs coupling of the two Ag NWs is more inclined to be distributed in the gap region. The gap distance between the two Ag NWs at point 1 is about 20 nm, and the enhancement factor of PL intensity is consistent with the simulation results.

In addition, the PL peaks of points 1 and 2 have different degrees of blue shift relative to the peak position of point 3. Since the points 1 and 2 are near the NWs, the blue shift of the peak position may be caused by the suspension of monolayer MoS_2 by Ag NWs [29]. The suspended monolayer MoS_2 is separated from the substrate to get rid of its n-type doping by SiO_2. The decrease of electron concentration in monolayer MoS_2 makes the luminescence of A exciton dominant, resulting in a blue shift of PL peak. In the Raman spectrum shown in Fig. 4c, it can be found that the baseline of the Raman spectrum at point 1 moves up as a whole, and its intensity is significantly higher than the other two points. This indicates that there is a significant light field enhancement effect in the gap-mode SPs of Ag NWs. From the change of the Raman peak position, it can be found that the A_{1g} peak position of point 1 (404.03 cm^{-1}) and 2 (403.81 cm^{-1}) have obvious blue shift relative to point 3. The ratio of A_{1g}/E^1_{2g} increases, while the peak position of E^1_{2g} does not change significantly, which is consistent with the Raman spectrum change of monolayer MoS_2 when doped with p-type [32]. Therefore, it also shows that the n-type electron doping of the substrate to the monolayer MoS_2 is avoided due to the suspension of the monolayer MoS_2 at points 1 and 2. Because both points 1 and 2 are near the nanowires, there are doping effects of silver nanowires on them, and the spectral intensity of point 1 is much higher than that of point 2, indicating that the main reason for the spectral enhancement of point 1 is still the field enhancement effect caused by the gap-mode SPs. In order to exclude the influence of other factors, we collected another Raman spectrum at similar points in Fig. 4c. The experimental results are shown in Fig. S1, which is similar to Fig. 4c, and the conclusion is verified again.

From the FDTD simulation results, it can be seen that the field strength of the SPs local light field in the gap mode of the double Ag NWs increases with the decrease of the gap distance within a certain range. However, the gap distance of the two parallel Ag NWs prepared above is still large, and the strong local light field cannot be excited. Therefore, the spectral enhancement of monolayer MoS_2 by two intersecting Ag NWs was also studied in the

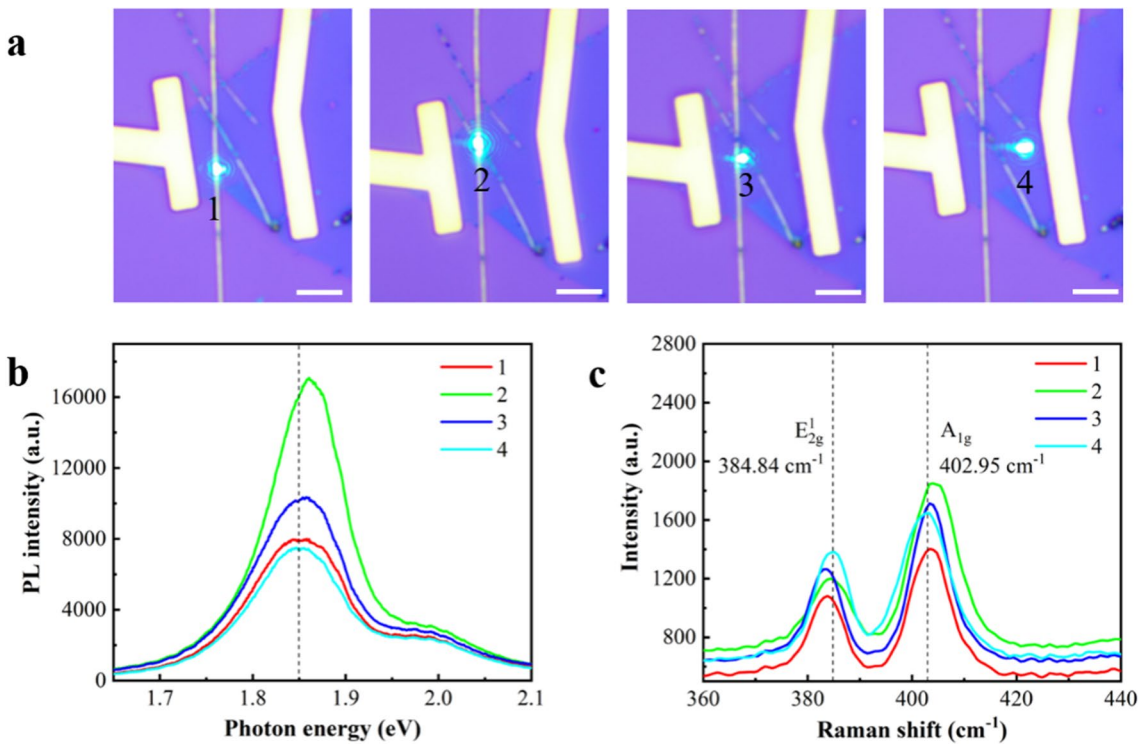

Fig. 5 Spectral enhancement of crossed Ag NWs in the MoS_2/Ag composite structure. **a** Locations of the spectrum collection points. All scales are 5 μm. **b** Comparison of PL spectra. **c** Comparison of Raman spectra

experiment. Figure 5a is the position of four spectral collection points. Point 1 is located on single Ag NW, point 2 is located at the intersection of double Ag NWs, point 3 is located on one side of the intersection and point 4 is located on monolayer MoS_2. The corresponding PL and Raman spectra are shown in Fig. 5b, c, respectively.

Compared with the pristine monolayer MoS_2, the PL peak intensity at point 1 is not significantly enhanced. Moreover, The PL intensity at point 2 is higher than that of point 3, indicating that the field strength of the local field increases with the decrease of the gap distance between the two Ag NWs. The above experimental results are consistent with the FDTD simulation results. The peak shift of points 1, 2 and 3 in Raman spectra also indicates that Ag NWs may cause p-type doping to monolayer MoS_2. In the comparison of Raman spectra, the E^1_{2g} peak positions at points 1 (383.87 cm^{-1}) and 3 (383.43 cm^{-1}) are red-shifted relative to point 4, which is consistent with the change of Raman spectra of monolayer MoS_2 under tensile stress [36]. It shows that the monolayer MoS_2 at these two points is subjected to a certain tensile stress due to being supported by Ag NWs. The presence of tensile stress reduces the PL intensity of monolayer MoS_2 [37]. In order to further demonstrate the solidity of the results, the Raman spectra of the similar positions of the four points in Fig. 5c are collected by increasing the laser power by 0.5 mW. As shown in Fig. S2, the intensity of the four Raman curves has increased, but the peak position and intensity relationship between them have not changed. Therefore, we believe that the experimental results are solid.

Under the influence of doping and stress, the spectral peak position of monolayer MoS_2 will shift in different situations, and the intensity of the spectrum can be modulated. It is necessary to exclude the influence of these factors on the spectral enhancement in order to prove that the main reason for the spectral enhancement of monolayer MoS_2 is the SPs of Ag NWs. In the experiment, Ag/MoS_2 composite structure was prepared by spin-coating Ag NWs directly on monolayer MoS_2 prepared by CVD method. When the Ag NWs is stacked on top of the MoS_2 film, it can be doped into the MoS_2 without causing tensile stress. Therefore, the influence of doping and stress on MoS_2 can be judged by comparing the difference of spectral enhancement in the two composite structures. As shown in Fig. 6a, two intersecting Ag NWs stacked on top of the MoS_2 are selected, and the PL and Raman spectra of four points are collected near them. Point 1 is located at the intersection of two NWs, point 2 is located on the side of the intersection of NWs, point 3

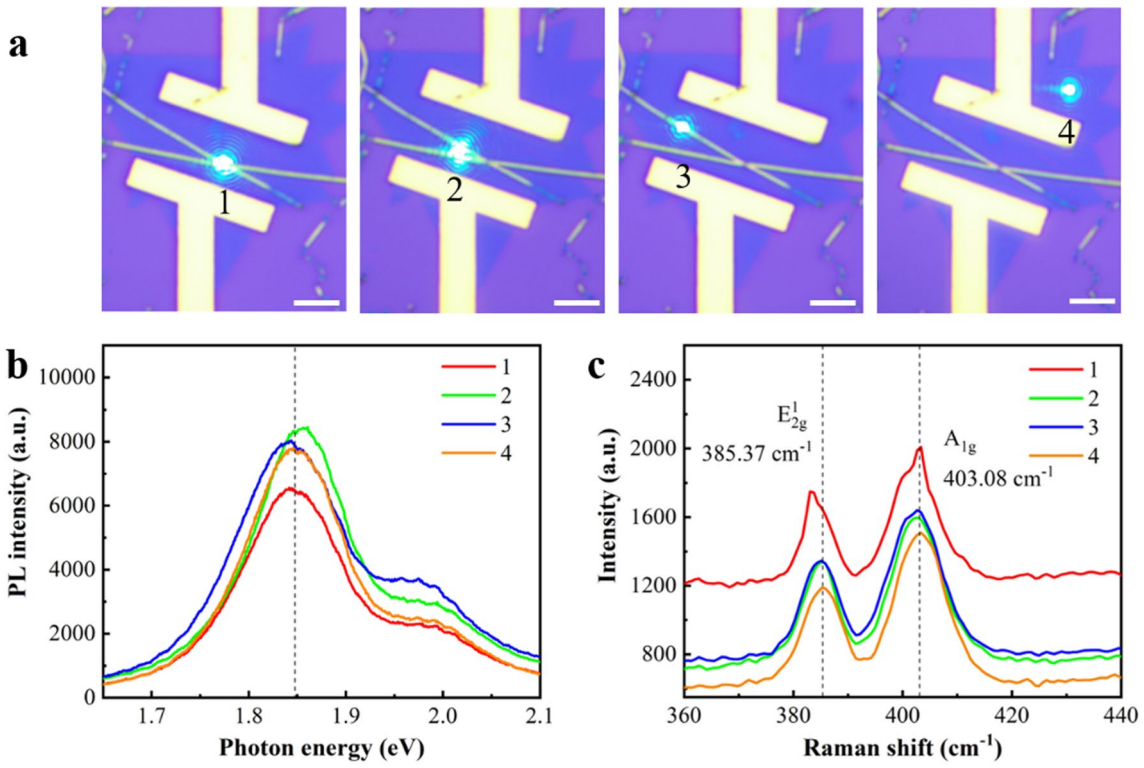

Fig. 6 Spectral enhancement of two intersecting Ag NWs in the Ag/MoS_2 composite structure. **a** Locations of the spectrum collection points. All scales are 5 μm. **b** Comparison of PL spectra. **c** Comparison of Raman spectra

is located on one of the NWs, and point 4 is located on the MoS_2 film.

When Ag NWs are stacked on the top layer, monolayer MoS_2 has low light field utilization for SPs. As shown in Fig. 6b, the PL spectra of each point has almost no spectral enhancement. On the same time, Ag NWs have an absorption and shielding effect on the spectral signal of the monolayer MoS_2. Especially near the intersection of the NWs, the overlapping Ag NWs almost completely block the MoS_2 film below, which reduces its PL intensity. As shown in Fig. 6c, although the Raman spectral intensity of each point is improved under the action of SPs, the spectral waveform of monolayer MoS_2 is distorted due to the interference of the above Ag NWs. In the spectra of Ag/MoS_2 composite structure, there is no obvious shift in the peak position of each point, which indicates that the p-type doping effect of Ag NWs on MoS_2 is not obvious. Therefore, doping is not the main reason for the spectral enhancement in the MoS_2/Ag composite structure. The presence of tensile stress tends to reduce the PL strength of MoS_2, which is inconsistent with the enhancement of PL strength in MoS_2/Ag composite structure. Hence, the effect of stress on the spectral enhancement of monolayer MoS_2 can also be excluded.

As a representative 2D semiconductor, monolayer MoS_2 can only absorb about 10% of visible light, which is not enough to achieve high photoelectric conversion efficiency. Using "gap mode" plasma to improve the photoelectric properties of 2D materials is one of the research hotspots in the field of 2D materials [25, 38, 39]. The gap-mode plasmonic composite structure designed in this work can effectively enhance the light-matter interaction of monolayer MoS_2, which provides a simple method for manufacturing low-cost and high-performance 2D material optoelectronic devices.

4 Conclusion

In summary, we use the FDTD method to simulate the local field enhancement of double Ag NWs gap-mode SPs at different gap distances. As the gap distance decreases, the coupled SPs electric field tends to concentrate in the gap of NWs, and the electric field enhancement coefficient is much higher than that of single Ag NW. In the MoS_2/Ag composite structure, by comparing the PL and Raman spectral intensity of monolayer MoS_2 in the gap and surrounding area, we verified that the local electric field of the double Ag NWs is mainly distributed in the gap. The experimental results are consistent with the fitting curve obtained by simulation. In addition, the effects of doping and stress on the experimental results were excluded by experiments on Ag/MoS_2 composite structure. These results provide a reference for the design of SPs nanostructures and the development of new optoelectronic devices.

Supplementary Information The online version contains supplementary material available at https://doi.org/10.1007/s00339-024-07403-z.

Acknowledgements The authors thank the support from the Jiangsu Agriculture Science and Technology Innovation Fund (No. CX(21)1007).

Author contributions Formal analysis, investigation: Weibin Zhang; Data curation: Cunwei Kong; Material characterization: Chunming Ji; Evaluation of results and editing: Xinfeng Zhang; Supervising, writing—review & editing: Quan Wang.

Data availability Data will be made available on request.

Declarations

Conflict of interest The authors have no conflicts of interest to declare that are relevant to the content of this article.

References

1. A. Abnavi, R. Ahmadi, H. Ghanbari et al., Flexible high-performance photovoltaic devices based on 2D MoS_2 diodes with geometrically asymmetric contact areas. Adv. Funct. Mater. **33**(7), 2210619 (2023)
2. Y.X. Sun, L.Y. Jiang, Z. Wang et al., Multiwavelength high-detectivity MoS_2 photodetectors with schottky contacts. ACS Nano **16**(12), 20272–20280 (2022)
3. K.F. Mak, C.G. Lee, J. Hone et al., Atomically thin MoS_2: a new direct-gap semiconductor. Phys. Rev. Lett. **105**(13), 136805 (2010)
4. A. Splendiani, S. Liang, Z. Yuanbo et al., Emerging photoluminescence in monolayer MoS_2. Nano Lett. **10**(4), 1271–1275 (2010)
5. O. Lopez-Sanchez, D. Lembke, M. Kayci et al., Ultrasensitive photodetectors based on monolayer MoS_2. Nat. Nanotechnol. **8**(7), 497–501 (2013)
6. A.C. Gomez, M. Barkelid, A.M. Goossens et al., Laser-thinning of MoS_2: on demand generation of a single-layer semiconductor. Nano Lett. **12**(6), 3187–3192 (2012)
7. M.H. Jeong, H.S. Ra, S.H. Lee et al., Multilayer WSe_2/MoS_2 heterojunction phototransistors through periodically arrayed nanopore structures for bandgap engineering. Adv. Mater. **34**(8), 2108412 (2022)
8. N. Li, C.L. He, Q.Q. Wang et al., Gate-tunable large-scale flexible monolayer MoS_2 devices for photodetectors and optoelectronic synapses. Nano Res. **15**(6), 5418–5424 (2022)
9. L.Q. Zhuo, D.Q. Li, W.D. Chen et al., High performance multifunction-in-one optoelectronic device by integrating graphene/MoS_2 heterostructures on side-polished fiber. Nanophotonics **11**(6), 1137–1147 (2022)
10. B. Radisavljevic, A. Radenovic, J. Brivio et al., Single-layer MoS_2 transistors. Nat. Nanotechnol. **6**(3), 147–150 (2011)
11. K.F. Mak, J. Shan, Photonics and optoelectronics of 2D semiconductor transition metal dichalcogenides. Nat. Photonics **10**(4), 216–226 (2016)
12. M. Bernardi, M. Palummo, J.C. Grossman, Extraordinary sunlight absorption and one nanometer thick photovoltaics using two-dimensional monolayer materials. Nano Lett. **13**(8), 3664–3670 (2013)
13. T. Laroche, A. Vial, M. Roussey, Crystalline structure's influence on the near-field optical properties of single plasmonic nanowires. Appl. Phys. Lett. **91**(12), 123101 (2007)

14. E. Hutter, J.H. Fendler, Exploitation of localized surface plasmon resonance. Adv. Mater. **16**(19), 1685–1706 (2004)
15. W.L. Barnes, A. Dereux, T.W. Ebbesen, Surface plasmon subwavelength optics. Nature **424**, 824–830 (2003)
16. A. Fratalocchi, C.M. Dodson, R. Zia et al., Nano-optics gets practical. Nat. Nanotechnol. **10**(1), 11–15 (2015)
17. Y. Zhang, W. Chen, T. Fu et al., Simultaneous surface-enhanced resonant Raman and fluorescence spectroscopy of monolayer $MoSe_2$: determination of ultrafast decay rates in nanometer dimension. Nano Lett. **19**(9), 6284–6291 (2019)
18. F. Cheng, A.D. Johnson, Y. Tsai et al., Enhanced photoluminescence of monolayer WS_2 on Ag films and nanowire-WS_2-film composites. ACS Photonics **4**(6), 1421–1430 (2017)
19. M.H. Tahersima, M.D. Birowosuto, Z. Ma et al., Testbeds for transition metal dichalcogenide photonics: efficacy of light emission enhancement in monomer vs dimer nanoscale antennae. ACS Photonics **4**(7), 1713–1721 (2017)
20. J. Lin, H. Li, H. Zhang et al., Plasmonic enhancement of photocurrent in MoS_2 field-effect-transistor. Appl. Phys. Lett. **102**(20), 203109 (2013)
21. Y. Li, M. Kang, J. Shi et al., Transversely divergent second harmonic generation by surface plasmon polaritons on single metallic nanowires. Nano Lett. **17**(12), 7803–7808 (2017)
22. Z. Wu, J. Yang, N.K. Manjunath et al., Gap-mode surface-plasmon-enhanced photoluminescence and photo response of MoS_2. Adv. Mater. **30**(27), 1706527 (2018)
23. B. Sun, Z. Wang, Z. Liu et al., Tailoring of silver nano-cubes with optimized localized surface plasmon in a gap mode for a flexible MoS_2 photodetector. Adv. Funct. Mater. **29**(26), 1900541 (2019)
24. P. Ni, A. Bugallo, V. Arreola et al., Gate-tunable emission of exciton-plasmon polaritons in hybrid MoS_2-gap-mode metasurfaces. ACS Photonics **6**(7), 1594–1601 (2019)
25. Q. Hao, J. Pang, Y. Zhang et al., Boosting the photoluminescence of monolayer MoS_2 on high-density nanodimer arrays with sub-10 nm gap. Adv. Opt. Mater. **6**(2), 1700984 (2018)
26. J. Miao, W. Hu, Y. Jing et al., Surface plasmon-enhanced photodetection in few layer MoS_2 phototransistors with Au nanostructure arrays. Small **11**(20), 2392–2398 (2015)
27. B. Lee, J. Park, G.H. Han et al., Fano resonance and spectrally modified photoluminescence enhancement in monolayer MoS_2 integrated with plasmonic nanoantenna array. Nano Lett. **15**(5), 3646–3653 (2015)
28. H.S. Lee, M.S. Kim, Y. Jin et al., Efficient exciton-plasmon conversion in Ag nanowire/monolayer MoS_2 hybrids: direct imaging and quantitative estimation of plasmon coupling and propagation. Adv. Opt. Mater. **3**(7), 943–947 (2015)
29. N. Scheuschner, O. Ochedowski, A.M. Kaulitz et al., Photoluminescence of freestanding single-and few-layer MoS_2. Phys. Rev. B **89**(12), 106–112 (2014)
30. S. Mouri, Y. Miyauchi, K. Matsuda, Tunable photoluminescence of monolayer MoS_2 via chemical doping. Nano Lett. **13**(12), 5944–5948 (2013)
31. Y. Sun, Z. Zhou, Z. Huang et al., Band structure engineering of interfacial semiconductors based on atomically thin lead iodide crystals. Adv. Mater. **31**(17), 1806562 (2019)
32. B. Chakraborty, A. Bera, D. Muthu et al., Symmetry-dependent phonon renormalization in monolayer MoS_2 transistor. Phys. Rev. B **85**(16), 396–404 (2012)
33. K. Kojima, H.E. Lim, Z. Liu et al., Restoring the intrinsic optical properties of CVD-grown MoS_2 monolayers and their heterostructures. Nanoscale **11**(27), 12798–12803 (2019)
34. M.S. Tame, K.R. Mcenery, ŞK. Özdemir et al., Quantum plasmonics. Nat. Phys. **9**(6), 329–340 (2013)
35. E. Cao, W. Lin, M. Sun et al., Exciton-plasmon coupling interactions: from principle to applications. Nanophotonics **7**(1), 145–167 (2018)
36. H.J. Conley, B. Wang, J.I. Ziegler et al., Bandgap engineering of strained monolayer and bilayer MoS_2. Nano Lett. **13**(8), 3626 (2013)
37. K. He, C. Poole, K.F. Mak et al., Experimental demonstration of continuous electronic structure tuning via strain in atomically thin MoS_2. Nano Lett. **13**(6), 2931–2936 (2013)
38. Z.Q. Wu, J.L. Yang, N.K. Manjunath et al., Gap-mode surface-plasmon-enhanced photoluminescence and photoresponse of MoS_2. Adv. Mater. **30**(27), 1706527 (2018)
39. H.Y. Lee, D. Nelson, W. Yan et al., Gap-surface plasmon-enhanced photoluminescence of InSe. Phys. Status Solidi B **260**(5), 2200436 (2023)